SEMARAK ILMU PUBLISHING

Semarak Journal of Thermal-Fluid Engineering

Journal homepage:
https://semarakilmu.com.my/journals/index.php/sjotfe/index
ISSN: 3030-6639

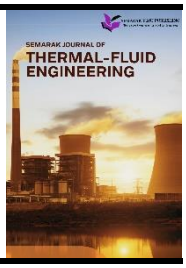

CFD Analysis of Different Baffles in Shell and Tube Exchanger

M. Saddam Kamarudin[1], Ishkrizat Taib[1,*], Muhammad Shaiful izzat Shaharudin[1], Muhammad Aiman Nasri[1], Muhammad Zulfaqar Mohd Madzni[1], Muhammad Nur Aiman Rahmat[1], Muhammadu Masin Muhammadu[2]

[1] Department of Mechanical Engineering, Faculty of Mechanical Engineering, Universiti of Tun Hussein Onn Malaysia, 86400 Parit Raja, Johor, Malaysia
[2] Faculty of Mechanical Engineering, Federal University of Technology, Minna (FUTMINNA), Nigeria

ARTICLE INFO

Article history:
Received 3 March 2024
Received in revised form 16 April 2024
Accepted 5 May 2024
Available online 1 June 2024

Keywords:
Shell-and-tube heat exchanger; baffle design; pressure drop; heat transfer; computational fluid dynamic

ABSTRACT

Shell and tube heat exchangers are among the most common equipment in industrial processes because of their heat exchange efficiency. However, designing these heat exchangers to enhance their performance can be cumbersome and time-consuming. This study focuses on evaluating the performance of shell and tube heat exchangers with different numbers of baffles placed inside the shell, and identifying the most suitable turbulence model. In this study, the flow characteristics inside the heat exchangers were modelled using three turbulence models: Spalart-Allmaras, k-ε standard, and k-ε realisable models. The simulations were performed with the number of baffles ranging from one to seven to understand their effect on heat transfer and pressure drop. When the number of baffles in the heat exchanger increases, the pressure drop across the heat exchanger also increases. Model D exhibited maximum pressure distribution, which occurred with 12 baffles. The velocity streamlines from the experiment showed that a higher number of baffles led to an increase in flow. This study also aimed to compare three turbulence models, and the results indicated that the k-ε realisable model performed the best of the three models. This study also highlights the importance of designing a shell and tube heat exchanger with an appropriate number of baffles. Although more baffling is advantageous for heat transfer, it also results in a higher pressure drop. In summary, as evidenced by the results presented in this paper, the baffle design is crucial for heat exchangers.

1. Introduction

In many industries, shell and tube heat exchangers (STEs) are the most common types of heat exchangers due to their heat transfer efficiency [1-2]. Counterflow is considered the most suitable flow arrangement for heat exchanger evaluation because of its compactness and design versatility [3-4]. Designing these heat exchangers involves complex relationships and equations, often requiring many iterations to determine the optimal solution [5]. It is easier to alter parameters related to heat transfer operations on the tube side, whereas making similar changes on the shell side can be time-

* *Corresponding author.*
E-mail address: iszat@uthm.edu.my

https://doi.org/10.37934/sjotfe.1.1.110

consuming. Computational Fluid Dynamics (CFD) has simplified this process by allowing visualisation of flow fields and temperatures, which aids in design improvements [6-7].

Baffles in heat exchangers are used to generate turbulence, which is crucial for improving heat transfer coefficients [8-9]. However, precautions must be taken when designing the baffles to ensure that the pressure drop in the shell-side fluid does not become excessively high [10]. Additionally, the baffles provided support to the tubes within the heat exchanger [11]. However, if a greater baffle spacing is used in the design of heat exchangers, flow-induced vibration can occur, potentially leading to tube failure [12-13].

A previous study focused on examining the STEs with different numbers of baffles to determine the most suitable turbulence model for implementation [14]. The method used in the previous study involved CFD simulation of a small-scale STE model, considering the aspects of geometry and meshing. Three turbulence models (Spalart-Allmaras, k-ε standard, and realisable k-ε) were used to study the flow characteristics inside the heat exchanger.

An earlier study revealed that the pressure drop increased with the number of baffles. The results showed that Model D with 12 baffles had the highest-pressure distribution. The velocity streamlines also indicated that higher baffle counts resulted in higher flow rates. This study further investigated the performance of the three turbulence models and found that the k-ε realisable model was the best [14].

Based on the observations from the previous study, the current work extends the investigation of STE performance with varying numbers of baffles. This research employs more sophisticated numerical methods and simulations to analyse the effect of baffles on heat transfer and pressure drop. Building on previous work, this study aims to provide a further understanding of STE design and ways to improve them for better industrial usage.

2. Methodology

A CFD simulation was conducted on a small lab-scale STE model to precisely visualise the heat transfer and pressure loss for the shell-side examination of the heat exchanger. Several geometric and design factors were considered for heat exchanger modelling.

2.1 Geometry of the Shell and Tube Exchanger

The geometry of the shell and tube heat exchanger (STE) features a shell diameter (Ds) of 90 mm, tubes with a diameter (Dt) of 20 mm, and a total of 7 tubes (Nt), as illustrated in Table 1. The heat exchanger has a length (L) of 600 mm, and the baffles are cut at 40% and 48%, with varying numbers of baffles (Nb) set at 6, 8, 10, and 12. The spacing between baffles (B) was 85.7 mm. These geometric parameters define the physical characteristics and operating conditions of the heat exchanger, which are crucial for the thermal performance analysis.

2.2 Mesh Generation

Mesh generation was conducted using the ANSYS Meshing software, employing a fine mesh with 273,429 elements, as shown in Figure 1. To ensure accurate results, the simulation was run on a progressively finer grid, adjusting the local refinements to assess the variations in the computational parameters.

Table 1
Geometrical parameters of the prototype

Parameter	Dimension
Shell Diameter, Ds	90 mm
Diameter of tube, Dt	20 mm
Tubes, Nt	7
Length of Heat Exchanger (HE), L	600 mm
Inlet temperature for shell side, Ts	300 K
Tube inlet temperature, Tt	450 K
Baffles cut, Bc	40% & 48%
Number of Baffles, Nb	6,8,10, &12
Baffle spacing, B	85.7 mm

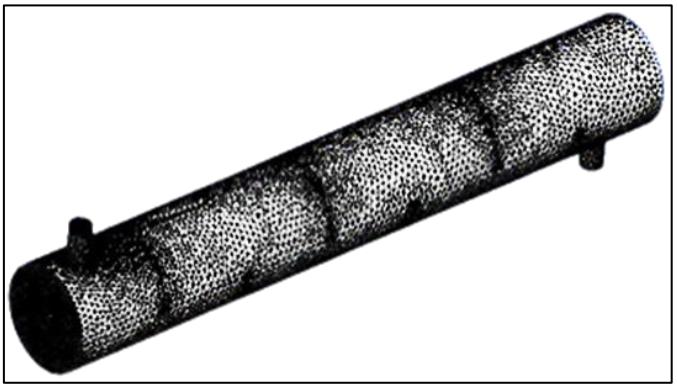

Fig. 1. Grid structure of shell and tube heat exchanger

2.3 Governing Equation for Shell and Tube Heat Exchanger

The governing equations for the flow inside a shell and tube heat exchanger are described by the Navier-Stokes equations, along with the equations for energy and turbulence modelling. The basic equations are as follows:

Continuity Equation:

$$\nabla . v = 0 \tag{1}$$

where v is the velocity vector.

Momentum Equation (Navier-Stokes Equation):

$$\rho \left(\frac{\delta v}{\delta t} + v . \nabla v\right) = -\nabla p + \mu \nabla^2 v + \rho g \tag{2}$$

where ρ is the fluid density, t is the time, p is the pressure, μ is the dynamic viscosity, and g is the gravitational acceleration vector.

Energy Equation:

$$\rho C_p \left(\frac{\delta T}{\delta t} + v . \nabla T\right) = \nabla . (\mathrm{k} \nabla \mathrm{T}) + \mathrm{Q} \tag{3}$$

where T is the temperature, Cp is the specific heat at a constant pressure, k is the thermal conductivity, and Q is the heat source/sink term.

2.3 Turbulence Modelling

The flow inside the heat exchanger is characterised by turbulence, necessitating the use of transient simulations and various turbulence models. In this study, three turbulence models were considered: the Spalart-Allmaras model, k-epsilon (k-ε) standard model, and k-epsilon realisable. The Spalart-Allmaras model relies on kinematic eddy viscosity and mixing length to define turbulent viscosity transport, making it efficient for specialised flows by solving a single transport equation [15-16]. The k–ε model is appropriate for scenarios in which convection and diffusion significantly affect turbulence. This model focuses on the turbulent kinetic energy mechanism [14-17]. The standard k–ε model is suitable for turbulent and non-separated flows, solving both turbulent kinetic energy and its dissipation rate, offering strong convergence, and serving as a general-purpose model. In contrast, the k-epsilon realisable model enhances the performance for complex geometries, resolves boundary layers using two-equation models, and is crucial for shell and tube analysis [18].

2.4 Boundary Conditions and Parameter Assumptions

The heat exchanger operates with an inlet temperature of 300 K for the shell side (Ts) and 450 K for the tube side (Tt). The critical boundary conditions for this small-scale STE model included the temperature and fluid flow rate at the intake. The desired boundary conditions in terms of the fluid flow rate and temperature were applied to achieve increased heat transfer with a minimal pressure drop at the output of the shell and tube. Details of the geometrical parameters are presented in Table 1. A no-slip condition was assigned to the surface and gravity was assigned to the Y-axis.

3. Results

3.1 The Grid Independent Test

A Grid Independence Test (GIT) was conducted to determine the optimal grid setup for the simulation. In this process, the cell size was gradually reduced to introduce more nodes and elements, thereby enhancing computational accuracy. Grid design plays a key role in determining the results derived from a CFD model, necessitating the identification of an ideal grid configuration. To establish the reliability, the same simulations were repeated five times using different settings. The results of the grid independence test are highlighted in Table 2, with test number 4 selected for all subsequent analyses and geometries. This test contained 50,810 nodes and 273,429 elements, representing a good balance between accuracy and computational costs. The computational geometry applications involved the use of tetrahedral meshing in the surface meshing, as shown in Figure 1.

Table 3 presents the results of the Grid Independence Test (GIT) for five test configurations: test number 1 (no. 1), test number 2 (no. 2), and test number 3 (no. 3), test number 4 (no. 4), and test number 5 (no. 5). Among these tests, test no. 4 is preferable to test no. 5 because it can perform simulations in a relatively short time span while utilising 50,810 nodes. Although test no. 5 provided the best accuracy with the highest number of nodes (115,810) and an orthogonal quality value nearest to 1 (0.77601, representing good quality on a scale of 0 to 1), test no. 4 remained acceptable with an orthogonal quality of 0.72521.

Table 2
Grid independent test for different setups

No	Node	Element	Skewness	Quality of Skewness	Orthogonal quality	Quality of orthogonal
1	17084	84754	0.31760	Very good	0.68131	Good
2	24102	123824	0.30210	Very good	0.69677	Good
3	30055	153944	0.28471	Very good	0.71417	Very good
4	50810	273429	0.27370	Very good	0.72521	Very good
5	115810	451821	0.22264	Excellent	0.77601	Very good

Table 3
Grid independent test

No	Node	Element	Skewness	Quality of Skewness	Orthogonal quality	Quality of orthogonal
1	17084	84754	0.31760	Very good	0.68131	Good
2	24102	123824	0.30210	Very good	0.69677	Good
3	30055	153944	0.28471	Very good	0.71417	Very good
4	50810	273429	0.27370	Very good	0.72521	Very good
5	115810	451821	0.22264	Excellent	0.77601	Very good

Moreover, test no. 5 was found to be the best in terms of skewness, with a value of 0.22264 (0 being the best and 1 being the worst) compared with test no. 4's skewness value of 0.27370. However, test no. 5 was considered less efficient due to its longer simulation time. The data collected indicated that as the number of nodes increased, so did the simulation time. Furthermore, it is worth emphasising that the numbers of elements and nodes are directly related. Figure 2 presents the correlations between skewness and orthogonal quality, showing that lower skewness corresponds to better orthogonal quality. Figure 3 demonstrates that a better orthogonal quality corresponds to higher accuracy.

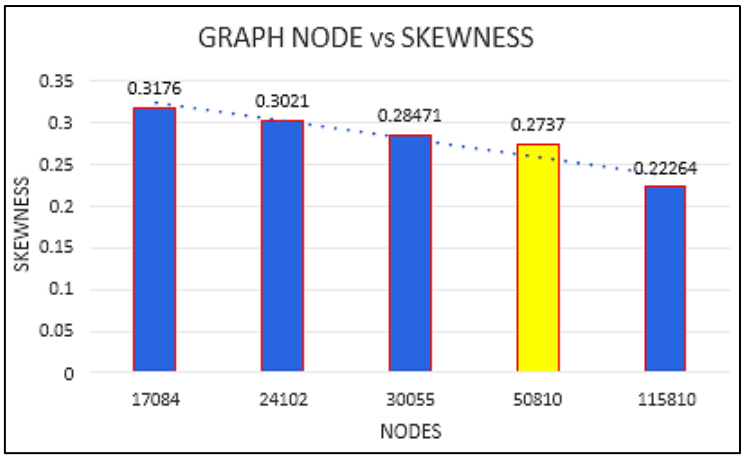

Fig. 2. Node vs Skewness graph

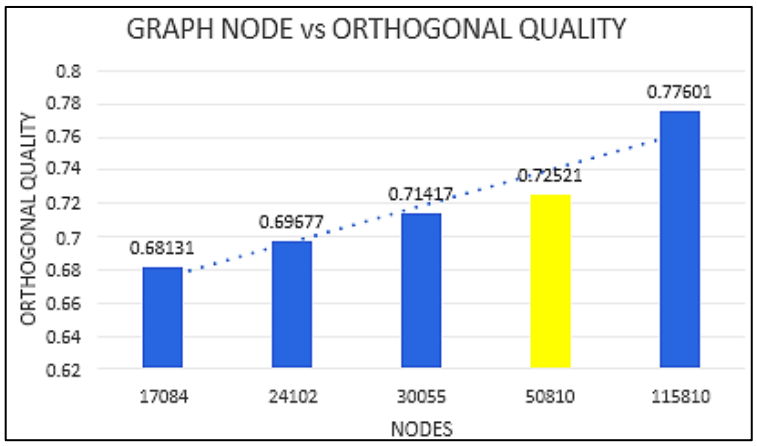

Fig. 3. Node vs orthogonal quality graph

3.1 Pressure Vector for all Models

This section discusses the pressure data obtained from simulations. The pressure for all the tests is presented as a pressure vector. In this simulation, four heat exchanger models with different numbers of baffles were analysed, each displaying distinct pressure behaviour patterns. Model A had six baffles, Model B had eight baffles, and Models C and D had 10 and 12 baffles, respectively. The pressure drop across the heat exchanger was calculated, which revealed the difference between the upstream and downstream pressures. This drop is typical because of the baffle spacing and cuts, which impede the fluid motion [19].

Following the determination of the appropriate turbulence model, simulations were conducted for the heat exchangers with 6, 8, 10, and 12 baffles. As shown in Table 4, the simulation results indicate that the pressure drop increased with the number of baffles. Additionally, the results highlight the optimal values for the baffle spacing and shell diameter ratio. Consequently, this study reveals previously unexplored relationships between the baffle spacing and heat exchanger geometry.

Table 4
Relation between baffle spacing and design parameter

Number of baffles	Central baffle spacing, B (mm)	Ratio of B/Ds
6	85.7	0.95
8	66.67	0.74
10	54.54	0.6
12	46.15	0.51

Figure 4 illustrates the pressure distributions against location for Models A, B, C, and D. It can be observed that the pressure at the inlet is higher than that at the outlet, with Model D exhibiting the highest pressure at several locations compared to Models A, B, and C. Conversely, Model A exhibited the lowest pressure distribution among the four models. At location 1, Model D shows the highest pressure at 609,270.06 Pa, whereas Models A, B, and C exhibit pressures of 174,559.22 Pa, 278,548.59 Pa, and 414,118.38 Pa, respectively. At location 2, Model A shows a slight increase in pressure from 174,559.22 Pa to 176,514.56 Pa, while Models B, C, and D demonstrate a decrease in pressure. From locations 3 to 9, the pressures for Models A, B, C, and D decreased consistently.

The pressure difference between two locations, known as the pressure drop, indicates that Model A has the lowest pressure drop at 161,577.73 Pa compared to Models B, C, and D, which have pressure drops of 227,206.39 Pa, 314,293.1 Pa, and 495,003.01 Pa, respectively. Table 5 presents the

pressure results at nine locations for all the four models. From these results, it is evident that Model A is the most efficient in maintaining a proper airflow in the system, as it requires the lowest pressure drop among the tested models.

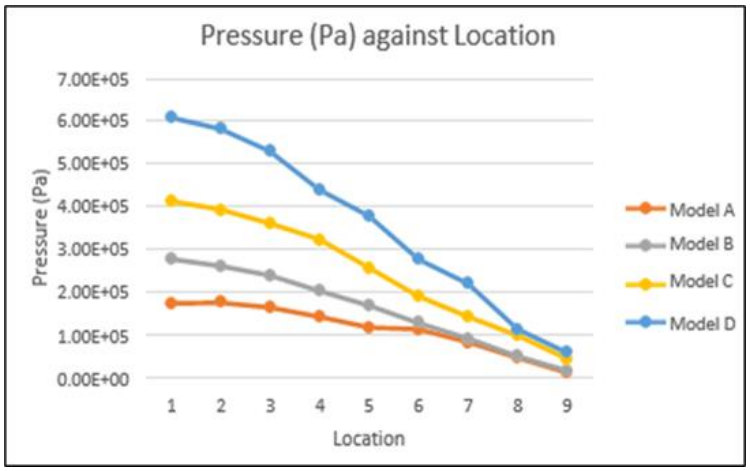

Fig. 4. Pressure profile for different location in heat exchanger

Table 5
Pressure result obtained from 9 locations on the system for all models

Location	Pressure (Pa)			
	Model A	Model B	Model C	Model D
1	174559.22	278548.59	414118.38	609270.06
2	176514.56	262470.84	394031.38	582766.75
3	165648.73	239978.09	361899.67	530430.88
4	143883.86	203622.53	324112.31	439885.94
5	118169.39	169808.20	258141.80	378313.31
6	114468.27	129382.27	191055.81	277749.94
7	83955.20	92951.10	143540.92	221019.55
8	47320.57	51342.20	99825.28	114267.05
9	12981.49	17002.00	45150.45	59117.55

3.2 Velocity Vector for all Models

The velocity distribution within the heat exchanger is represented by velocity streamlines, which illustrate the flow pattern in the system. Figure 5 presents the velocity vectors for all heat exchanger models, with simulations performed at a mass flow rate of 0.5 kg/s for varying numbers of baffles. It was observed that the water changed direction upon encountering the baffle plates, thereby creating an effective crossflow within the heat exchanger. In Models C and D, a recirculation zone is briefly visualised, as shown in Figure 5. This suggests that the flow was well developed and recirculation was possible. These simulations indicate that heat exchangers with 10 and 12 baffles exhibit a more effective and acceptable design.

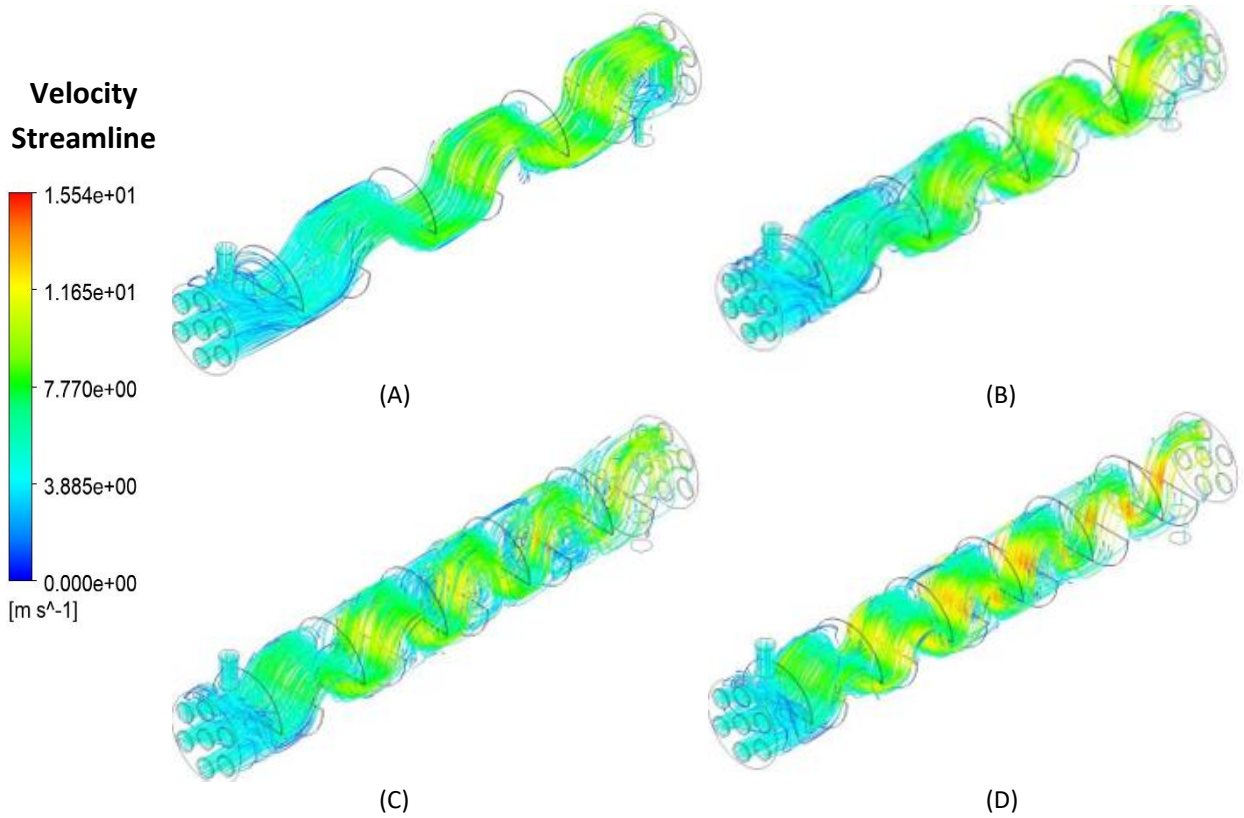

Fig. 5. Velocity streamlines for Model A with 6 number of baffles, Model B with 8 number of baffles, Model C with 10 number of baffles, Model D with 12 number of baffles

3.3 Discussion

A recent CFD simulation study selected a few baffle configurations for the comparison and validation of the present CFD model, as shown in Table 3. Various design parameters, such as the number of baffles, baffle cut (BC), and baffle spacing, were adjusted to study different output parameters, such as pressure drop, heat transfer coefficient, and total heat transfer. The results showed that an increase in the fluid flow rate led to an increase in the pressure at the output. Conversely, a pressure drop is common owing to the baffle spacing and cuts that impede fluid flow. Some methods employed to enhance the shell-side performance include the modification of the thermal and transport characteristics and design specifications [20].

The investigation was performed using appropriate mesh density, discretisation, and turbulence modelling, as the low-pressure aspects of shell-side calculations are problem dependent. The k–ε realisable model with 1st order discretization approach emerged as the best among the three turbulent models tested. The simulation followed the same process for all CFD enquiries concerning this matter.

Following an increase in the number of baffles, the new geometry was re-meshed in ANSYS and the simulation was conducted accordingly. As the baffle spacing was reduced, both the heat transfer and the pressure drop increased. The pressure drop values increased proportionally with the fluid flow. Design parameters such as baffle spacing (ranging from 6 to 12 baffles) and baffle cut were adjusted for three distinct fluid flow rates. The baffle cut significantly influenced fluid-to-fluid heat transfer, with a 50% baffle cut yielding superior outcomes compared with lower percentages.

Reduced baffle cuts led to the formation of recirculation zones behind the baffles, which impeded the full utilisation of the crossflow windows when using a total of 12 baffles. This issue was mitigated by increasing the baffle cut and adding more baffles, demonstrating that a 50% baffle cut enhances

the performance of the heat exchanger. Lower mass flow rates resulted in smaller percentage differences for the configurations with 6, 8, and 10 baffles. It was observed that increasing the baffle spacing within the shell improved the overall heat transfer for this single-segmental baffle design heat exchanger. In addition, the pressure drop increased with higher flow rates.

4. Conclusions

The investigation conducted in this study utilised a computational model to evaluate and compare the efficiency of the shell side of a Shell and Tube Heat Exchanger (STE), supported by a literature review. This study aims to improve the shell-side performance by altering the thermal and transport characteristics of the shell and adjusting design parameters. Given that the pressure contours on the shell side are crucial for shell-side calculations, this study employed appropriate mesh density, discretisation, and turbulence modelling. The baffle had a significant impact on the heat transfer between the fluids, with a 50% baffle cut providing the best performance. This means that fewer baffle cuts were used to create recirculation zones behind the baffles, thus limiting the use of crossflow windows. A correlation-based approach could also supplement the current CFD-based analysis to provide more evidence to support the conclusions drawn. Among all models, Model D exhibited the highest velocity streamline at a velocity of 1.554 m/s. Therefore, it can be concluded that a higher number of baffles leads to a higher streamline velocity.

Acknowledgment

This research was supported by Universiti Tun Hussein Onn Malaysia (UTHM) through Tier 1 (vot Q542).

References

[1] Mohanty, Shuvam, and Rajesh Arora. "CFD analysis of a shell and tube heat exchanger with single segmental baffles." *International Journal of Automotive and Mechanical Engineering* 17, no. 2 (2020): 7890-7901. http://dx.doi.org/10.15282/ijame.17.2.2020.08.0589

[2] Alzahmi, Ahmed, Mohammed Alswat, W. A. El-Askary, and Khaled Ramzy. "Harvesting waste-heat energy of shell and tube heat exchanger used for desalination purposes using thermoelectric power generation modules: Numerical studies." *International Communications in Heat and Mass Transfer* 156 (2024): 107569. https://doi.org/10.1016/j.icheatmasstransfer.2024.107569

[3] Gupta, Sanjeev Kumar, Harshita Verma, and Neha Yadav. "A review on recent development of nanofluid utilization in shell & tube heat exchanger for saving of energy." *Materials Today: Proceedings* 54 (2022): 579-589. https://doi.org/10.1016/j.matpr.2021.09.455

[4] Prasad, Arjun Kumar, and Kaushik Anand. "Design and analysis of shell and tube type heat exchanger." *International Journal of Engineeering research and Technology* 9, no. 1 (2020): 524-539.

[5] Klemeš, Jiří Jaromír, Qiu-Wang Wang, Petar Sabev Varbanov, Min Zeng, Hon Huin Chin, Nathan Sanjay Lal, Nian-Qi Li, Bohong Wang, Xue-Chao Wang, and Timothy Gordon Walmsley. "Heat transfer enhancement, intensification and optimisation in heat exchanger network retrofit and operation." *Renewable and Sustainable Energy Reviews* 120 (2020): 109644. https://doi.org/10.1016/j.rser.2019.109644

[6] Mohammadzadeh, A. M., Bahram Jafari, and Khashayar Hosseinzadeh. "Comprehensive numerical investigation of the effect of various baffle design and baffle spacing on a shell and tube heat exchanger." *Applied Thermal Engineering* 249 (2024): 123305. https://doi.org/10.1016/j.applthermaleng.2024.123305

[7] Saijal, Kizhakke Kodakkattu, and Thondiyil Danish. "Design optimization of a shell and tube heat exchanger with staggered baffles using neural network and genetic algorithm." *Proceedings of the Institution of Mechanical Engineers, Part C: Journal of Mechanical Engineering Science* 235, no. 22 (2021): 5931-5946. https://doi.org/10.1177/09544062211005797

[8] Abbasian Arani, Ali Akbar, and Hamed Uosofvand. "Improving shell and tube heat exchanger thermohydraulic performance using combined baffle." *International Journal of Numerical Methods for Heat and Fluid Flow* 30, no. 8 (2020): 4119-4140. https://doi.org/10.1108/HFF-06-2019-0514

[9] Ribeiro, Fabio, Kevin E. de Conde, Ezio Castejon Garcia, and Idario P. Nascimento. "Heat transfer performance enhancement in compact heat exchangers by the use of turbulators in the inner side." *Applied Thermal Engineering* 173 (2020): 115188. https://doi.org/10.1016/j.applthermaleng.2020.115188

[10] Azimy, Hamidreza, Amir Homayoon Meghdadi Isfahani, Masoud Farahnakian, and Arash Karimipour. "Experimental investigation of the effectiveness of ultrasounds on increasing heat transfer coefficient of heat exchangers." *International Communications in Heat and Mass Transfer* 127 (2021): 105575. https://doi.org/10.1016/j.icheatmasstransfer.2021.105575

[11] Marzouk, S. A., M. M. Abou Al-Sood, Emad MS El-Said, M. M. Younes, and Magda K. El-Fakharany. "A comprehensive review of methods of heat transfer enhancement in shell and tube heat exchangers." *Journal of Thermal Analysis and Calorimetry 148,* no. 15 (2023): 7539-7578. https://doi.org/10.1007/s10973-023-12265-3

[12] Marzouk, S. A., M. M. Abou Al-Sood, Magda K. El-Fakharany, and Emad MS El-Said. "A comparative numerical study of shell and multi-tube heat exchanger performance with different baffles configurations." *International Journal of Thermal Sciences* 179 (2022): 107655. https://doi.org/10.1016/j.ijthermalsci.2022.107655

[13] Thulukkanam, Kuppan. *Heat Exchangers: Operation, Performance, and Maintenance.* CRC Press, 2024. https://doi.org/10.1201/9781003352068

[14] Varaksin, Aleksey Yu, and Sergei V. Ryzhkov. "Turbulence in two-phase flows with macro-, micro-and nanoparticles: A review." *Symmetry* 14, no. 11 (2022): 2433. https://doi.org/10.3390/sym14112433

[15] Li, Wenhao, and Yangwei Liu. "Numerical investigation of corner separation flow using Spalart-Allmaras model with various modifications." *Aerospace Science and Technology* 127 (2022): 107682. https://doi.org/10.1016/j.ast.2022.107682

[16] Aliabadi, Amir A. "Turbulent-Viscosity Models." In *Turbulence: A Fundamental Approach for Scientists and Engineers* (2022): 195-209. https://doi.org/10.1007/978-3-030-95411-6_15

[17] Avila, Marc, Dwight Barkley, and Björn Hof. "Transition to turbulence in pipe flow." *Annual Review of Fluid Mechanics* 55 (2023): 575-602. https://doi.org/10.1146/annurev-fluid-120720-025957

[18] Santos, Humberto, Wei Li, and David Kukulka. "Numerical study of thermal-hydraulic performance improvement of enhanced surface tubes." *Heat Transfer Engineering 44*, no. 2 (2023): 103-124. https://doi.org/10.1080/01457632.2022.2034082

[19] Al-Mansori, Nassrin Jassim Hussien, Thair Jabbar Mizhir Alfatlawi, Khalid S. Hashim, and Laith S. Al-Zubaidi. "The effects of different shaped baffle blocks on the energy dissipation." *Civil Engineering Journal* 6, no. 5 (2020): 961-973. https://dx.doi.org/10.28991/cej-2020-03091521

[20] Abbasian Arani, Ali Akbar, and Hamed Uosofvand. "Improving shell and tube heat exchanger thermohydraulic performance using combined baffle." *International Journal of Numerical Methods for Heat & Fluid Flow 30*, no. 8 (2020): 4119-4140. https://doi.org/10.1108/HFF-06-2019-0514